Title: Evaluation of a three-dimensional ultrasound localisation system incorporating probe pressure correction for use in partial breast irradiation

Harris EJ, Symonds-Taylor R, Treece GM, Gee AH, Prager RW, Brabants P, Evans PM

Abstract

This work evaluates a 3D freehand ultrasound-based localisation system with new probe pressure correction for use in partial breast irradiation. Accuracy and precision of absolute position measurement was measured as a function of imaging depth (ID), object depth, scanning direction and time, using a water phantom containing crossed wires. To quantify the improvement in accuracy due to pressure correction, 3D scans of a breast phantom containing ball bearings were obtained with no pressure and with pressure. Ball bearing displacements were measured with and without pressure correction. Using a single scan direction, for all imaging depths, mean error was < 1.3mm, with the exception of the wires at 68.5mm imaged with ID = 85mm which gave a mean error of -2.3mm. Precision was > 1mm for any single scan direction, this fell to 1.7mm for multiple scan directions. Probe pressure corrections of between 0mm and 2.2mm have been observed for pressure displacements of 1.1mm to 4.2mm. Overall, AP position measurement accuracy increased from 2.2mm to 1.6mm and to 1.4mm for the two opposing scanning directions. Precision is comparable to that reported for other commercially available ultrasound localisation systems provided 3D image acquisition is performed in the same scan direction. The existing temporal calibration is imperfect and a per-installation calibration would further improve the accuracy and precision. Probe pressure correction was shown to improve the accuracy and will be useful in the localisation of the excision cavity for partial breast radiotherapy.

1. Introduction

Partial breast irradiation is used to deliver dose to the excision cavity post conservative breast surgery. The excision cavity is defined as the clinical target volume and may be localised for patient set up using imaging techniques. Soft tissue imaging techniques include cone beam computed tomography [1], megavoltage computed tomography [2] and ultrasound [3]. Other techniques include fiducial markers, such as surgical clips or implanted markers, combined with kilovoltage [4] or megavoltage X-ray imaging [5].

All of these methods rely on the identification of a surrogate for the excision cavity. The soft tissue imaging methods are no exception, both CBCT and ultrasound use the presence of seroma to identify the excision cavity [6]. Clips have been shown to be strong surrogates for the excision cavity and are reported to be the gold standard [7]. However there is the possibility of clip migration [8] and clips are difficult to see in portal images and therefore additional kV x-ray imaging is required.

A number of 3D ultrasound-based localisation systems are now commercially available including BAT (Nomos, Chatsworth, USA), Restitu (Resonant Medical, Montreal, Canada) and SonArray (Varian, Palo Alto, USA) which give improved visualisation of soft tissue when compared to conventional X-ray imaging. These systems have mainly been used for prostate localisation. The precision and accuracy with which ultrasound can be used to locate the prostate has been shown to be limited by probe pressure [9] and observer error [1]. The Restitu^{TM} Clarity^{TM} (Resonant Medical, Montreal, Canada) has recently been introduced for the localisation of the

excision cavity. To the best of our knowledge no studies using this system for excision cavity localisation for patient set-up have been published. Only the latter system is based upon freehand 3D ultrasound image acquisition, the others use dedicated 3D probes.

A new commercially available system which has been developed specifically for localisation in breast radiotherapy is Orpheus (Qados Ltd., Surrey, UK) which is based upon a freehand 3D ultrasound system [10]. Similar to the above systems, the user acquires a 3D ultrasound scan of the target volume which is placed in the treatment room frame-of-reference and allows the user to identify the 3D position co-ordinates of the target relative to the treatment isocentre. An evaluation of the initial system based upon 3D localisation software, has previously been undertaken [11] in which relative-position measurements of spheres in a phantom were carried out to determine the geometrical accuracy and precision of the system. Coles et al. [12] evaluated the localisation of the centre of mass of excision cavity measured using Orpheus by comparison with CT. Subsequently this system has been adapted to work in any clinical radiotherapy setting and now has the facility to correct for probe pressure artefacts. This latter improvement would seem to be essential to any ultrasound based breast localisation system, given the proximity of the excision cavity to the skin. Treece et al. have described their probe pressure correction algorithm in detail and qualitatively demonstrated improvements in images subject to probe pressure artefacts [13]. Prior to clinical application of this system to excision cavity localisation for patient set-up we wish to verify the absolute positional accuracy of the system in the treatment room and to quantify the improvement in position accuracy afforded by probe pressure correction. To do this we have conducted two phantom

based experimental studies, the details and results of which are the subject of this paper. The aims of these studies were to evaluate the Orpheus system for use in partial breast irradiation in two stages:

- Firstly, the accuracy and precision of the absolute position measurement of points within a water phantom were measured.
- Secondly, probe pressure correction was evaluated by measuring the positions of objects in a breast phantom before and after probe pressure correction.

2. Methods

This section describes the Orpheus localisation system, the phantoms used to evaluate accuracy and precision and probe pressure correction, the experimental method and the parameters investigated.

2.1 Orpheus localisation system

The Orpheus system is designed such that it can be used with most clinical ultrasound scanners and 2D probes. We used an Accuvix XQ ultrasound scanner (Medison Co., Ltd, Seoul, S. Korea) to acquire ultrasound images. The L5-12IM ultrasound probe used is a linear array transducer of frequency 5MHz ~12MHz. The probe has a range of imaging depth from 30mm to 85mm. A passive Polaris (Northern Digital Inc. Ontario, Canada) position sensor was rigidly attached to the ultrasound probe. To acquire freehand 3D data the Orpheus system requires a personal computer and frame grabber to capture video data of the B-scan image display from the ultrasound scanner whilst simultaneously acquiring 3D position information from Polaris. For initial set-up 3 calibrations are necessary: temporal calibration, spatial calibration and isocentre

calibration. Temporal calibration is required to determine the offset between the position sensor time-stamps and the B-scan time-stamps [11]. To reduce the complexity of the user-performed set-up procedure, the system incorporates a "one-size-fits-all" temporal calibration which is not performed by the user. Spatial calibration is necessary to determine the size and location of the B-scan imaging plane relative to the position sensor. A spatial calibration must be performed for each imaging depth (ID) that will be used. Three imaging depths were chosen for these experiments. These were the minimum and maximum imaging depths available, 30mm and 85mm and a medium imaging depth of 50mm. A single transmit focus positioned at half of the imaging depth was used for all experiments. Each spatial calibration was carried out using the procedure described by Treece at al. [11] which took approximately 10 minutes to perform. Position vectors to transform the Polaris co-ordinate system to the treatment room co-ordinate system were acquired using an isocentre calibration. The isocentre calibration was performed by aligning a box phantom of known dimensions with the treatment room lasers. The Polaris pointer was used to point to known positions on the box and the positions indicated by the pointer were captured by the Orpheus system. Hence, all positions measured using the Orpheus systems are relative to the treatment room isocentre.

2.2 Phantoms

Two phantoms were used to evaluate the system. The first was a 15cm × 15cm × 15cm Perspex tank that can be filled with water (see figure 1). Eighteen Perspex wires were threaded across the tank at three different distances from the top of the tank. The wires were arranged such that they cross each other perpendicularly i.e. the crossing points were of minimal size. The position of the wire crossings with respect to the

centre of the tank was known with a precision of 0.5mm. The centre of the tank was aligned with the treatment room laser isocentre using crosshairs marked on the tank with a precision of 0.5mm. At the beginning of each experiment the tank was filled with water that was approximately 48° centigrade. This is the temperature at which the speed of sound in water is $1540ms^{-1}$, the speed of sound assumed by the ultrasound scanner [14].

The second phantom, which was used to evaluate the probe pressure correction, was a breast biopsy phantom (CIRS inc., Virginia, USA). This phantom was manufactured from tissue mimicking material Zerdine®. To create point targets within the phantom eight 0.5mm diameter ball bearings were inserted into the phantom using a biopsy needle. It was necessary to acquire 3D scans with both zero pressure and pressure and therefore, in order to more easily acquire zero pressure 3D scans of the breast phantom, the phantom was placed inside the water tank.

2.3 Position acquisition

The wire crossings were imaged by scanning the probe across the surface of the water. Four scanning directions were investigated: superior to inferior (SI), inferior to superior (IS), right to left (RL) and left to right (LR). Three freehand 3D scans of the water tank were acquired for each imaging depth and for each scanning direction. The positions of the wire crossings were identified manually in each 3D scan using the Orpheus software for the identification of landmarks. To assess the stability of the system repeat acquisitions were made 3 and 5 months later. The temperature of the water was monitored and recorded throughout the experiments and the anterior to posterior (AP) positions of the wire crossings were corrected as described by

Goldstein et al. [15] for change in the speed of sound due to the fall in temperature of the water.

The efficacy of the probe pressure correction was assessed as follows. Twelve 3D ultrasound image acquisitions of the breast phantom in water were obtained with zero probe pressure in the SI direction. The positions of the ball bearings were identified in each of the 3D scans and the mean positions and depths from the surface of the phantom were determined. When a contact ultrasound scan was performed, pressure was applied shortly after the start of the scan and then maintained throughout the scan. The probe pressure correction uses the first few images of the ultrasound scan just before pressure is applied to correct the images obtained with pressure, i.e. if the scan acquisition starts after pressure is applied there are no zero pressure images with which to compare the pressure images. To investigate the probe pressure correction as a function of distance from the start of the scan 12 scans were also acquired in the IS direction so that ball bearings of different depths were close to the start of the scan. Inter-observer error associated with manually locating the wire crossings and the ball bearings in the 3D images was assessed by making 10 repeat measurements of positions of the 3 wire crossings and a single ball bearing (obtained using zero pressure 3D scans). The deepest wire crossings and ball bearing were chosen to represent the worst case: spatial resolution decreases with depth below the foci.

2.4 Parameters investigated

The position measurement accuracy and precision, uni-dimensionally, of the Orpheus system was evaluated as a function of

- Depth of target

- Imaging depth
- Scanning direction
- Time

The probe pressure correction was evaluated as a function of

- Distance from the start of the scan
- Depth of target.

3. Results

3.1 Observer error

The inter-observer error in the left-right (LR), superior-inferior (SI) and anterior-posterior (AP) directions are given in table 1 for the two phantoms. For all directions and both phantoms inter-observer error is less than 0.5mm

3.2 Accuracy and precision as a function of depth and imaging depth

Tables 2, 3 and 4 give the accuracy and precision as a function of depth in the LR, AP and SI directions for 30mm, 50mm and 85mm imaging depths respectively, for 3 repeat scans in the SI direction. For all imaging depths, mean error was less than 1.1mm and 1.3mm for the SI and LR directions respectively, with the exception of the wires at 68.5mm imaged with ID = 85mm which gave a mean error of -2.3mm (corresponding to the inferior direction). For ID = 85mm, which can be used to visualise all wires, the precision was greatest at 33.5mm which was the depth closest to the transit and elevational foci.

Figure 2 gives the mean error and precision (error bars) for position measurements of wire crossings at a depth of 13.5mm as a function of ID for the SI scanning direction. This plot show the differences between the 3D positions measured using the different IDs. These differences are largest in the AP direction (2.4mm between ID = 50mm and ID = 85mm). All AP positions (i.e. depths) have been corrected for changes in the speed of sound due to the fall in water temperature. The poor accuracy in the AP direction therefore suggests the presence of errors in the spatial calibrations of the ultrasound probe.

3.4 Accuracy as a function of scan direction

Figure 3 gives a plot of the mean positions of wire crossings at 13.5mm measured using a 50mm imaging depth. The true positions of the wires are indicated by the diagonal lines and their intersections are shown by diamond markers. For the SI scanning direction, the measured positions are slightly inferior (-1mm), while for scanning in the IS direction measured positions are superior (+1.3mm) of the true positions. Measured left/right positions do not change significantly when the scanning direction is changed from SI to IS. Error bars are not shown as precision was found to be less than 0.53mm (1 SD) in the scanning direction and 0.2mm in the direction perpendicular to the scanning direction. The same behaviour is observed for LR and RL scanning where measured positions are right and left of the actual positions respectively. This is consistent with an imperfect temporal calibration.

Table 5 summarises the accuracy and precision (1SD) for each of the scanning directions and imaging depths investigated for wires at all depths. Only the LR and SI position measurements are given because AP positions are not affected by changing

the scanning direction. For each imaging depth the standard deviation in the mean position if all directions are considered is given. The results show a decrease in precision if multiple scan directions are used i.e. the SD of the SI position for the ID = 50mm is 1.97mm for multiple directions compared to a maximum SD of 0.53mm for a single direction. Similar observations can be made if we consider wires at greater depths, however, the wires at 13.5mm have been presented here because these can be imaged using all three imaging depths.

3.5 Stability

The standard deviation of the mean errors (and precision) measured in months 1, 4 and 6 were greatest for an imaging depth of 85mm. These were 0.15mm (0.22mm), 0.72mm (0.17mm) and 0.6mm (0.42mm), indicating that the system remained stable over a five month period.

3.6 Probe pressure

Figure 4 gives the measured depth of the eight ball bearings inserted into the breast phantom from the surface of the phantom as a function of the distance of the ball bearing from the start of the scan, i.e. the point at which pressure is initially applied. From figure 5 we can see that application of pressure decreases the depth of the ball bearing relative to the case where no pressure is applied. Applying the probe pressure correction re-adjusts the position of the ball bearings away from the surface, i.e. they move towards their true depth. From figure 5(a) the distance by which the depth is corrected is greater for ball bearings at the beginning of the scan. This is also seen in figure 5(b) with the exception of the deepest ball bearing. The maximum and minimum depth displacement due to probe pressure was 4.2 and 1.1mm respectively.

Mean probe pressure correction (and standard deviation) was 0.5mm (0.5mm) and 0.8mm (0.7mm) for the SI and IS scans respectively. The maximum and minimum probe pressure corrections measured were 2.16mm and 0.01mm respectively. No correlation between the magnitude of displacement due to pressure and the magnitude of the pressure correction was observed.

4. Discussion

A number of 3D ultrasound localisation systems for application to radiotherapy have been previously evaluated. Bouchet et al. [16] evaluated a system based on a dedicated 3D probe (Medison, Pleasanton, CA) using a phantom containing 15 echoic spheres. The position accuracy was found to be < 1.2mm and the precision (SD) < 0.7mm at a depth of 60mm. Tome et al. [17] also evaluated the target localisation accuracy of a dedicated 3D probe based guidance system (SonArray^{TM}, ZMed, Inc. MA) using a similar ultrasound phantom containing 12 echoic spheres and an IR fiducial array. Accuracy of this system was reported to be between 0.1mm to 1.6mm with SD between 0.05mm to 0.8mm for depths of up to 70mm. Both of these systems are designed for localisation of the prostate and use 3D probes that mechanically "sweep out" a volumetric image of tissue. Neither of these studies varies the orientation of the 3D probe. A more recent study evaluates the Restitu^{TM} system. The accuracy with which the system could determine the position of objects within the manufacturer-provided quality assurance phantom was less than 2.1 mm (SD = 0.8 mm) by Drever and Hilts [18]. In comparison to these studies, the accuracy with which the position of the wire crossings could be located in the present study is poorer in the scanning direction (up to 2.9 mm for ID = 50mm). This can be attributed to a non-perfect temporal calibration, i.e. there is residual time-delay between the transfer

of the probe position co-ordinates from the Polaris and the corresponding image frame. This is supported by the observation that the mean error in the scan direction changes sign if the scan direction is rotated through 180°. We would expect this error to decrease with decreasing scanning speed, i.e. the speed at which the probe is moved across the surface of the patient. If we consider the accuracy in the non-scan direction there are mean errors of up 2.3mm at a depth of 68.5mm which are comparable to that reported for other systems.

The precision of the Orpheus system (~1mm SD) was found to be comparable with other systems if scanning is restricted to one direction and to one imaging depth. Precision decreases if we scan in multiple directions due to change in mean error resulting from the imperfect temporal calibration. For systems which use dedicated 3D probes the probe remains stationary during image acquisition and therefore any error in temporal calibration will not create a positional error. However, error in the spatial calibration will alter the precision of the system if probe orientation is changed. The precision of the systems described above [16-18] as a function of 3D probe orientation has not been reported upon and therefore any direct comparison for multiple scan directions is not possible. Rather than restrict imaging protocol to one direction, a per-installation temporal calibration should be preformed to reduce these temporal calibration errors and scanning should be performed as slowly as possible. The next version of Orpheus will incorporate a facility for the user to tailor the temporal calibration to their particular installation and therefore these results should be viewed as lower bounds on what can be achieved without these improvements made to the temporal calibration.

Evaluation of the probe pressure correction using the breast phantom has shown that the correction increases the accuracy with which the ball bearings can be located. Probe pressure corrections of between 0mm and 2.16mm have been observed for pressure displacements of 1.12mm to 4.23mm. The amount of displacement of tissue due to probe pressure will depend on many factors, including the depth of tissue and the elasticity of the breast and therefore it is difficult to predict the range of displacements we can expect. However breast tissue will have increased heterogeneity compared with the breast phantom used for this experiment and this is expected in clinical practice to increase the efficacy of the probe pressure correction which relies on the cross-correlation of neighbouring imaging images [11]. From the results it is expected that the pressure correction will increase the accuracy of the system to locate tissue within the breast.

5. Conclusions

We have evaluated a breast localisation system which incorporates probe pressure correction. The accuracy of the system is less than 3mm and the precision within 1mm provided the scanning is reproducible, i.e. the same scanning direction is used. Thus, we have identified the need for a per-installation temporal calibration. The precision of the system is comparable to that reported for other commercially available ultrasound localisation systems. The probe pressure correction was shown to improve the accuracy with which objects could be located within a breast biopsy phantom. Corrections of up to 2.2mm were observed for probe pressure displacements of up to 4.2mm. These results show that the probe pressure correction will be useful in the localisation of the excision cavity for partial breast radiotherapy.

Table captions

Table 1. Inter-observer error for measured wire crossing positions in the water phantom (scanning direction = LR) and for ball bearing positions in the breast phantom (scanning direction = SI).

Table 2. Accuracy and precision (1 SD) for position measurements in the LR, AP and SI directions as a function of depth for an imaging depth of 30mm and transit focus at 20mm (scanning direction = SI).

Table 3. Accuracy and precision (1 SD) for position measurements in the LR, AP and SI directions as a function of depth for an imaging depth of 50mm and transit focus at 25mm (scanning direction = SI).

Table 4. Accuracy and precision (1 SD) for position measurements in the LR, AP and SI directions as a function of depth for an imaging depth of 85mm and transit focus at 40mm (scanning direction = SI).

Table 5. Accuracy and precision (1SD) as a function of scanning direction for 30mm, 50mm and 85mm imaging depths and precision across all scan directions for all depths.

Figure captions

Figure 1. Schematic diagram of the water phantom used to assess accuracy and precision.

Figure 2 Mean error and precision (error bars) for wire crossings at a depth of 13.5mm as a function of imaging depth (scanning direction = SI).

Figure 3 Plot of mean measured positions of wire crossings at a depth of 13.5mm (imaging depth = 50mm) for the SI, IS, LR and RL scan directions. True position of the wires is shown by diagonal lines and crossing positions are shown by diamond markers.

Figure 4 Plot of ball bearing depth measured without probe pressure, with probe pressure and corrected positions scanning in (a) the SI direction and (b) the IS direction. Measurement precision is indicated for each distance by error bars on pressure data points.

References

1. van Herk M. Different styles of image-guided radiotherapy. Seminars in Radiation Oncology2007 Oct;17(4):258-67.

2. Langen KM, Buchholz DJ, Burch DR, Burkavage R, Limaye AU, Meeks SL, et al. Investigation of accelerated partial breast patient alignment and treatment with helical tomotherapy unit. International Journal of Radiation Oncology Biology Physics2008;70(4):1272-80.

3. Ringash J, Whelan T, Elliott E, Minuk T, Sanders K, Lukka H, et al. Accuracy of ultrasound in localization of breast boost field. Radiotherapy and Oncology2004 Jul;72(1):61-6.

4. Kinoshita R, Shimizu S, Taguchi H, Katoh N, Fujino M, Onimaru R, et al. Three-dimensional intrafractional motion of breast during tangential breast irradiation monitored with high-sampling frequency using a real-time tumor-tracking radiotherapy system. International Journal of Radiation Oncology Biology Physics2008 Mar;70(3):931-4.

5. Coles CE, Wishart G, Donovan E, Harris E, Poynter A, Twyman N, et al. The IMPORT gold seed study: Evaluation of tumour bed localisation and image-guided radiotherapy for breast cancer. Clinical Oncology2007;19(3):S26-S7.

6. Kass R, Kumar G, Klimberg VS, Kass L, Henry-Tillman R, Johnson A, et al. Clip migration in stereotactic biopsy. American Journal of Surgery2002;184(4):325-31.

7. Goldberg H, Prosnitz RG, Olson JA, Marks LB. Definition of postlumpectomy tumor bed for radiotherapy boost field planning: CT versus surgical clips. International Journal of Radiation Oncology Biology Physics2005;63(1):209-13.

8. Birdwell RL, Jackman RJ. Clip or marker migration 5-10 weeks after stereotactic 11-gauge vacuum-assisted breast biopsy: Report of two cases. Radiology2003;229(2):541-4.

9. McGahan JP, Ryu J, Fogata M. Ultrasound probe pressure as a source of error in prostate localization for external beam radiotherapy. International Journal of Radiation Oncology Biology Physics2004;60(3):788-93.

10. Prager RW, Gee A, Berman L. Stradx: real-time acquisition and visualization of freehand three-dimensional ultrasound. Med Image Anal1999;3(2):129-40.

11. Treece GM, Gee AH, Prager RW, Cash CJC, Berman LH. High-definition freehand 3-D ultrasound. Ultrasound in Medicine and Biology2003;29(4):529-46.

12. Coles CE, Cash CJC, Treece GM, Miller F, Hoole ACF, Gee AH, et al. High definition three-dimensional ultrasound to localise the tumour bed: A breast radiotherapy planning study. Radiotherapy and Oncology2007;84:233-41.

13. Treece GM, Prager RW, Gee AH, Berman L. Correction of probe pressure artifacts in freehand 3D ultrasound. Medical Image Analysis2002;6(3):199-214.

14. Bilaniuk N, Wong GSK. SPEED OF SOUND IN PURE WATER AS A FUNCTION OF TEMPERATURE. Journal of the Acoustical Society of

America1993;93(3):1609-12.

15. Goldstein A. The effect of acoustic velocity on phantom measurements. Ultrasound in Medicine and Biology2000;26(7):1133-43.

16. Bouchet LG, Meeks SL, Bova FJ, Buatti JM, Friedman WA. Three-dimensional ultrasound image guidance for high-precision extracranial radiosurgery and radiotherapy. Radiosurgery, Vol 42002;4:262-78.

17. Tome WA, Meeks SL, Orton NP, Bouchet LG, Bova FJ. Commissioning and quality assurance of an optically guided three-dimensional ultrasound target localization system for radiotherapy. Medical Physics2002;29(8):1781-8.

18. Drever L, Hilts M. Experiences with the quality assurance testing of the restitu ultrasound system. Medical Physics2006;33(7):2672-.

Figure 1

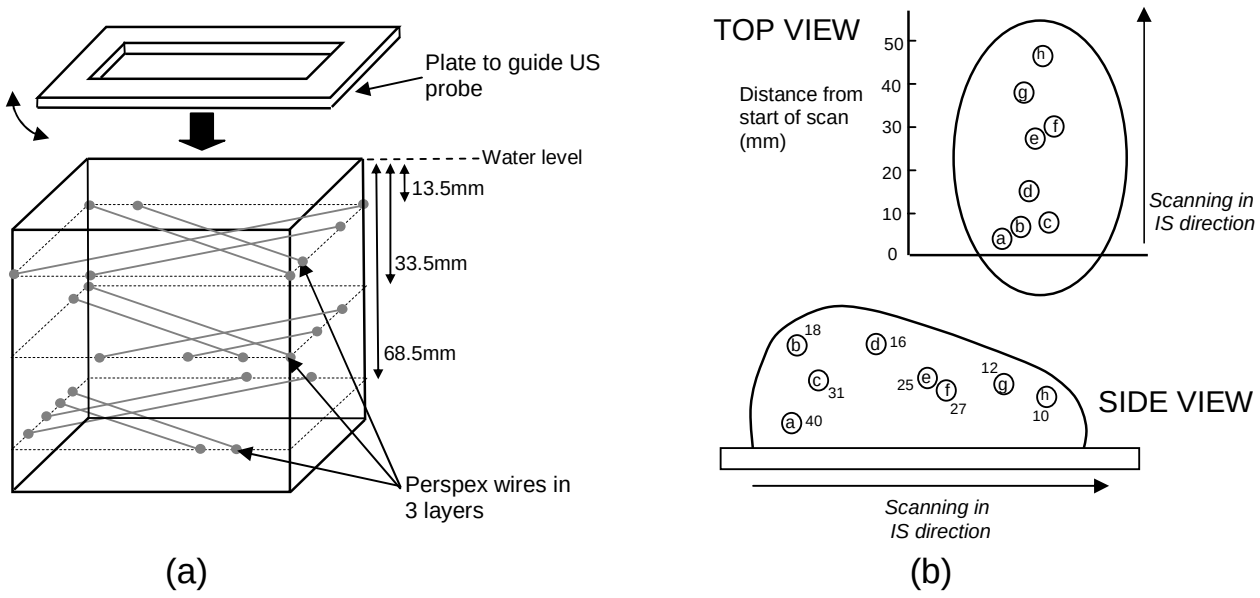
Plate to guide US probe
Water level
13.5mm
33.5mm
68.5mm
Perspex wires in 3 layers
(a)
TOP VIEW
Distance from start of scan (mm)
50
40
30
20
10
0
h
g
f
e
d
b
c
a
Scanning in IS direction
b 18
d 16
c 31
e 25
f 27
g 12
h 10
a 40
SIDE VIEW
Scanning in IS direction
(b)

Figure 2

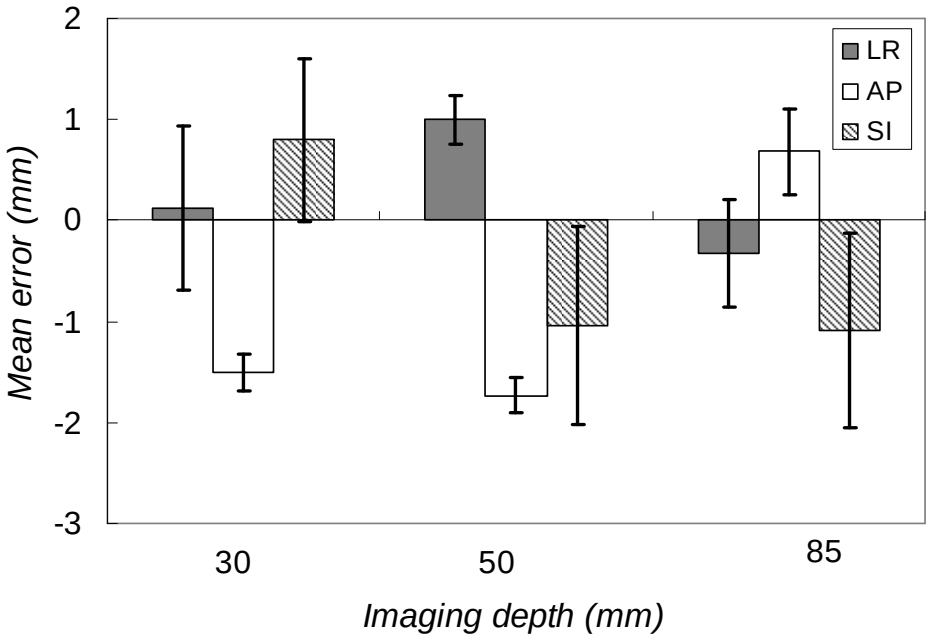

Figure 3

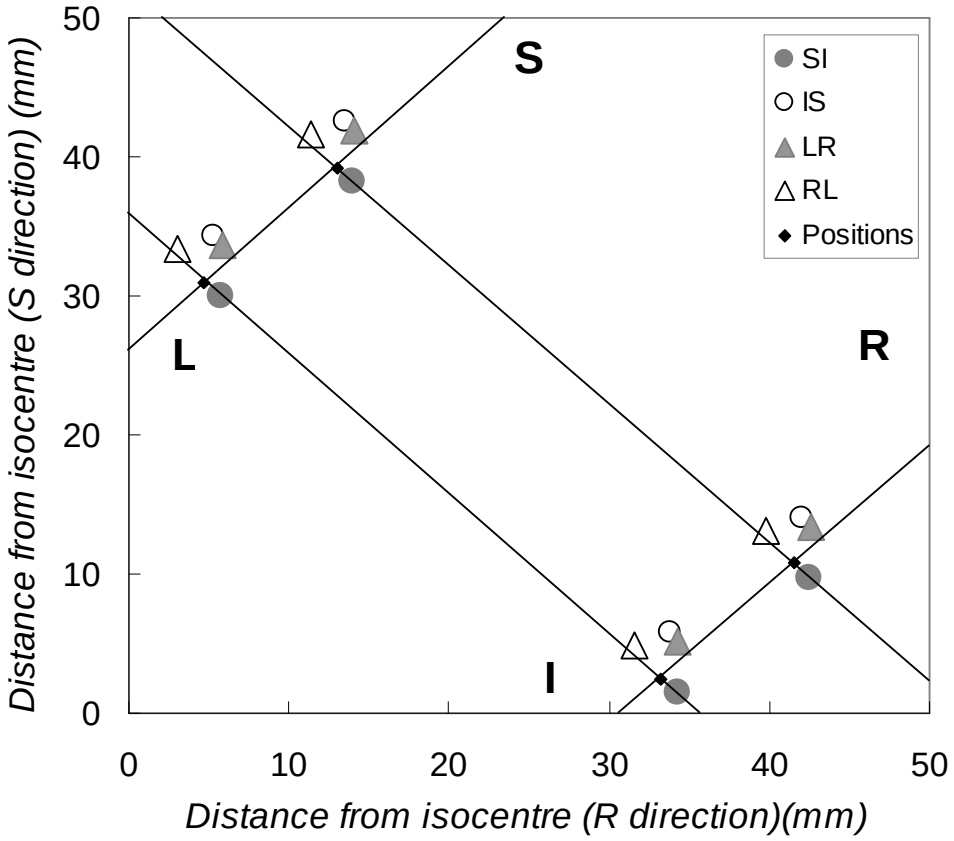
S
L
R
I
SI
IS
LR
RL
Positions
Distance from isocentre (S direction) (mm)
Distance from isocentre (R direction)(mm)
0
10
20
30
40
50

Figure 4

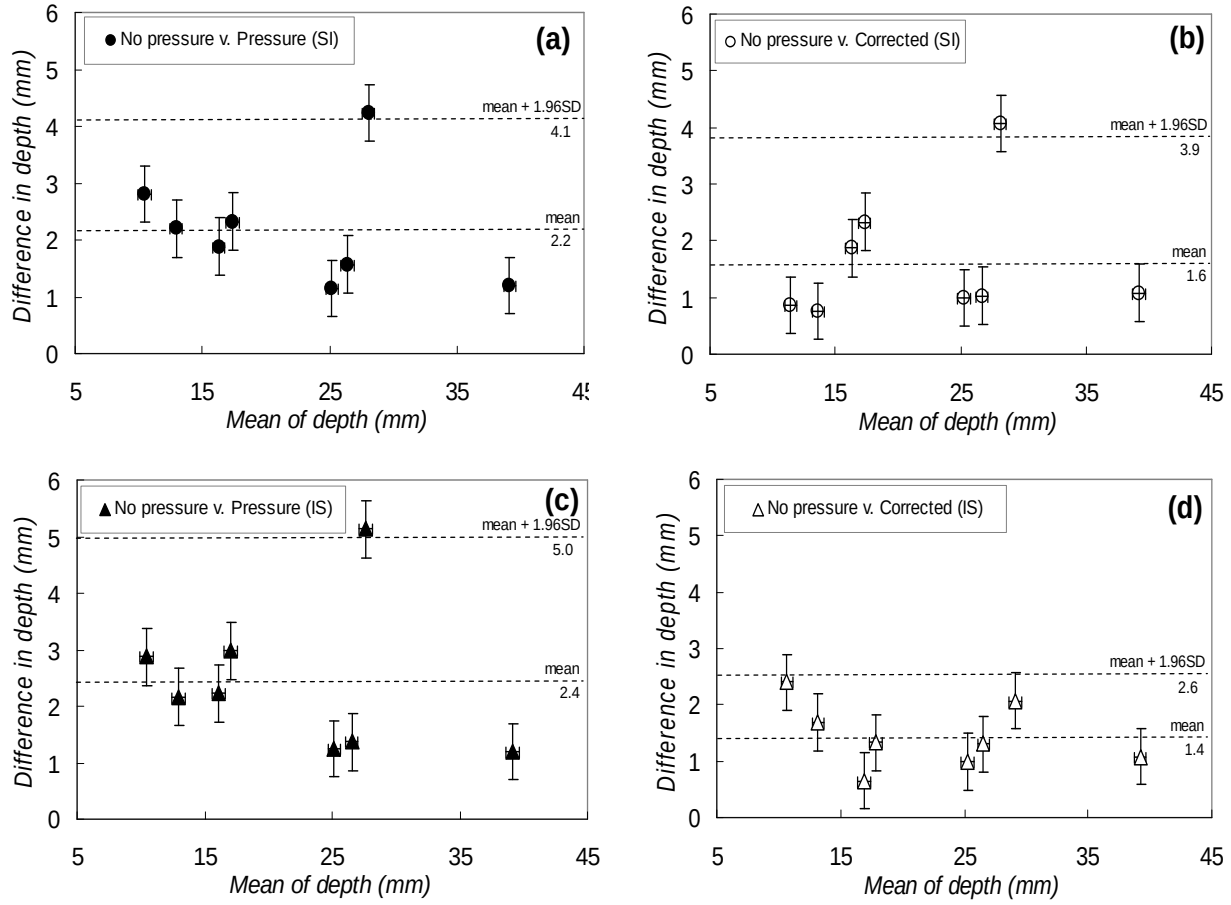
● No pressure v. Pressure (SI)
(a)
mean + 1.96SD
4.1
mean
2.2
Difference in depth (mm)
Mean of depth (mm)
○ No pressure v. Corrected (SI)
(b)
mean + 1.96SD
3.9
mean
1.6
▲ No pressure v. Pressure (IS)
(c)
mean + 1.96SD
5.0
mean
2.4
△ No pressure v. Corrected (IS)
(d)
mean + 1.96SD
2.6
mean
1.4

Table 1

Phantom	Intra-observer error (Coefficient of repeatability) (mm)		
	LR	AP	SI
Water	0.8	0.7	0.2
Breast	0.4	0.3	0.4

Table 2

Depth (mm)	LR (mm)	AP (mm)	SI (mm)
13.5	0.1 ± 0.8	-1.5 ± 0.2	0.8 ± 0.8

Table 3

Depth (mm)	LR (mm)	AP (mm)	SI (mm)
13.5	1.0 ± 0.2	-1.8 ± 0.2	-1.0 ± 1.0
33.5	1.2 ± 0.3	-1.7 ± 0.3	-0.9 ± 1.0
All depths	1.1± 0.3	-2.0 ± 0.2	-1.0 ± 0.9

Table 4

Depth (mm)	LR (mm)	AP (mm)	SI (mm)
13.5	-0.3 ± 0.5	0.7 ± 0.4	-1.1 ± 0.7
33.5	-1.0 ± 0.4	0.9 ± 0.1	-1.1 ± 0.5
68.5	-1.3 ± 0.5	0.4 ± 0.3	-2.3 ± 0.9
All depths	-0.8 ± 0.6	0.6 ± 0.4	-1.6 ± 1.0

Table 5

Scanning direction	Accuracy and Precision (all depths) (mm)					
	30		50		85	
	LR	SI	LR	SI	LR	SI
SI	0.1 ± 0.8	0.8 ± 0.8	1.0 ± 0.3	-1.0 ± 0.9	-0.8 ± 0.6	-1.6 ± 1.0
IS	0.0 ± 0.4	2.9± 0.6	0.6 ± 0.5	2.9 ± 0.9	0.0 ± 0.7	2.7 ± 1.0
LR	1.5 ± 0.7	0.2 ± 0.4	0.9 ± 0.5	2.0 ± 0.7	2.4 ± 1.0	1.2 ± 0.6
RL	-1.8 ± 0.6	0.1 ± 0.3	-1.5 ± 0.6	2.3 ± 0.5	-2.3 ± 0.4	1.2 ± 0.7
SD (all directions)	**0.6**	**1.3**	**1.1**	**1.6**	**1.7**	**1.6**